

## Effect of Glow-discharge Hydrogen Plasma Treatment on Zinc Oxide Layers Prepared through Pulsed Electrochemical Deposition and via SILAR Method

N.P. Klochko<sup>1</sup>, K.S. Klepikova<sup>1,\*</sup>, S.I. Petrushenko<sup>2</sup>, A.V. Nikitin<sup>3</sup>, V.R. Kopach<sup>1</sup>, I.V. Khrypunova<sup>1</sup>, D.O. Zhadan<sup>1</sup>, S.V. Dukarov<sup>2</sup>, V.M. Lyubov<sup>1</sup>, A.L. Khrypunova<sup>1</sup>

<sup>1</sup> National Technical University "Kharkiv Polytechnic Institute", 2, Kyrpychov St., 61002 Kharkiv, Ukraine

<sup>2</sup> V.N. Karazin Kharkiv National University, 4, Svobody Square, 61022 Kharkiv, Ukraine

<sup>3</sup> National Science Center "Kharkov Institute of Physics & Technology", 1, Academichna St., 61108 Kharkiv, Ukraine

(Received 07 May 2019; revised manuscript received 21 October 2019; published online 25 October 2019)

In this work, we investigated the effect of glow-discharge  $H_2^+$  plasma treatment on ZnO layers deposited on fluorine doped tin oxide (FTO) glass substrates through low temperature aqueous solution growth, namely, via a pulsed electrochemical deposition and by successive ionic layer adsorption and reaction (SILAR) technique. It is shown that the crystal structure, surface morphology, chemical composition and optical properties obtain some destructive changes after plasma processing due to the creation of oxygen vacancies  $V_o$  and H-related defects, and additionally, because of the zinc oxide etching by the glow-discharge  $H_2^+$  plasma through reduction of zinc oxide and evaporation of Zn from the surface. Nevertheless, our investigations show quite good stability of the ZnO layers to the plasma-induced radiation and chemical impacts under high total  $H_2^+$  fluence received by every ZnO/FTO sample  $\sim 8 \cdot 10^{18} \text{ cm}^{-2}$ .

**Keywords:** Glow discharge, Zinc oxide, Pulse electrodeposition, SILAR, Hydrogen plasma treatment.

DOI: [10.21272/jnep.11\(5\).05002](https://doi.org/10.21272/jnep.11(5).05002)

PACS number: 81.40.Wx

### 1. INTRODUCTION

Hydrogen plasma treatment has many potential applications for a modern technology of microelectronic and optoelectronic devices based on zinc oxide (ZnO) thin films and nanostructures [1-9]. In addition, in the interplanetary space hydrogen molecules along with electrons and ions, especially  $H_2^+$  ions, are the components of the solar wind plasma [10], so the space plasma interacts with spacecraft materials, including zinc oxide coatings, which are subjected to a number of different destructive and non-destructive processes. Space radiation is a great danger to electronics onboard space vessels. Therefore, an understanding of the mechanisms of damage in the ZnO contained electronics, solar cells and other devices is critical to spacecraft construction and operational anomaly resolution.

Among the various ways to create hydrogen plasma, a glow discharge is distinguished by its use in a large number of application fields, such as in the microelectronics industry and in the plasma displays, and also in the materials technology of solar cells and various kinds of light sources [11, 12]. However, we were unable to detect information in the literature concerning the effects of the direct current (DC) glow-discharge hydrogen plasma on zinc oxide films or nanostructures. According to [11], the glow-discharge hydrogen plasma is a partially ionized gas consisting of nearly equal concentrations of positive and negative charges and a large number of neutral species. The DC glow discharge formed in a cell filled with  $H_2$  at low pressure is created by applying a potential difference between two electrodes. Owing to the potential difference,  $H_2$  atoms are ionized to yield free electrons and positively charged ions that is called "gas breakdown". The positive ions are accelerated towards the cathode of the glow discharge, where they can release electrons upon bombardment called "secondary electron emission". The electrons

arrive in the plasma, and can give rise to collisions with the gas particles, the most important collisions being excitation and ionization of these gas particles [11]. The ionization collisions create new ions and electrons. The ions can again release electrons from the cathode material; the electrons can, in turn, give rise to new ionization collisions creating new ion-electron pairs. This electron-ion multiplication process makes the glow discharge a self-sustaining plasma.

In this work, we investigated the effect of glow-discharge  $H_2^+$  plasma treatment on ZnO layers deposited through low temperature aqueous solution growth, namely, via a pulsed electrochemical deposition and by successive ionic layer adsorption and reaction (SILAR) technique. These methods have become very popular in recent years [13, 14] because they allow ZnO deposition over large areas and suggest low capital expenditure based on simple process equipment. As substrates we used glass sheets covered with transparent conductive  $SnO_2:F$  film (FTO coated glass plates TEC 7, Pilkington Company, USA). In this way, we prepared ZnO/FTO samples. Morphology of ZnO layers, both before and after their glow-discharge  $H_2^+$  plasma treatment, was observed by scanning electron microscopy (SEM). Chemical composition of the ZnO/FTO samples was investigated by X-ray fluorescence (XRF) microanalysis. Impact of the glow-discharge  $H_2^+$  plasma on ZnO optical properties has been examined by means of spectrophotometry. To research crystal structure we used X-ray diffraction (XRD) method.

### 2. EXPERIMENTAL DETAILS

We prepared two types of ZnO/FTO samples for research. The first one was grown via a pulsed electrochemical deposition, and the other ZnO/FTO sample was obtained by SILAR technique.

\* [catherinakle@gmail.com](mailto:catherinakle@gmail.com)

For the electrochemical deposition of ZnO layer in the form of one-dimensional (1D) array we used a standard thermostatic three-electrode electrochemical cell with platinum spring as counter-electrode and saturated Ag/AgCl reference electrode in unstirred aqueous electrolyte containing 0.01 M  $\text{Zn}(\text{NO}_3)_2$  and 0.1 M  $\text{NaNO}_3$  on FTO substrate. Temperature of the electrolyte was 70 °C. Firstly, ZnO seed layer was formed via potentiostatic electrochemical deposition provided by a programmable impulse potentiostat PI-0.5-1.1 during short time (30 s) at potential  $U = -1.3$  V (here and below, vs. Ag/AgCl). After that, a plating of 1D ZnO was carried out in the same electrolyte during 15 min in the pulsed mode by applying rectangular potential pulses. The lower and upper potential limits were, respectively,  $U_{\text{off}} = -0.7$  V and  $U_{\text{on}} = -1.3$  V. A duty cycle ( $D_c = 0.4$ ) was given as relation  $T_{\text{on}}/(T_{\text{on}} + T_{\text{off}})$ , where  $T_{\text{on}}$  is a time at potential  $U_{\text{on}}$ , and  $T_{\text{off}}$  is a time at potential  $U_{\text{off}}$ . Potential pulse frequency  $f$  was 2 Hz. As a result, 1D ZnO array with average thickness ( $t$ ), which corresponds to the length of nanorods,  $t \approx 0.7$   $\mu\text{m}$ , was grown on FTO surface.

To prepare ZnO/FTO sample by means of SILAR method, the deposition of ZnO film on FTO substrate was carried out during 100 SILAR deposition cycles using aqueous solution 0.8 M  $\text{NH}_4\text{OH}$  and 1 M  $\text{ZnSO}_4$  as cationic precursor. In this SILAR process, one growth cycle included following three steps: (1) immersing the substrate into cationic precursor for 10 s; (2) immersing of FTO immediately into anionic precursor, namely into hot (90 °C) water for 10 s; (3) its rinsing in a separate  $\text{H}_2\text{O}$  beaker at room temperature for 5 s to remove loosely bound particles. The obtained ZnO film has thickness  $t \approx 1$   $\mu\text{m}$ .

For the hydrogen plasma treatment of zinc oxide layers, the glow-discharge self-sustaining  $\text{H}_2^+$  plasma was generated in DC mode at 1 keV energy. A potential difference 1 kV was created between anode and uncoated part of ZnO/FTO sample (FTO substrate) used as cathode.  $\text{H}_2^+$  current density was 1.5 mA/cm<sup>2</sup> with cathode voltage  $-1$  kV. All plasma treatments of ZnO layers were performed for 15 min each. Total  $\text{H}_2^+$  fluence received by every ZnO/FTO sample was  $\sim 8 \cdot 10^{18}$  cm<sup>-2</sup>.

Morphology of the ZnO layers both before and after hydrogen plasma treatment was observed by SEM in a secondary electron mode. The SEM instrument "Tescan Vega 3 LMH" operated at an accelerating voltage 30 kV without the use of additional conductive coatings.

Elemental analysis of ZnO/FTO samples was carried out by X-ray fluorescence microanalysis using an energy dispersive spectrometry (EDS) system "Bruker XFlash 5010". Energy dispersion spectra were taken from the 50×50  $\mu\text{m}$  sample areas. Quantification of the spectra was carried out in the self-calibrating detector mode.

Optical properties of ZnO layers were studied in the wavelength range 300-1100 nm with an SF-2000 spectrophotometer equipped with SFO-2000 reflection attachment for a registration of diffuse reflection spectra  $R_d = f(\lambda)$ . FTO substrates were used as control samples when optical transmission spectra  $T_o(\lambda)$  were recorded. Optical band gaps  $E_g$  of ZnO were determined from absorption coefficients  $\alpha$  calculated as described in [15]:

$$\alpha = 1/t \cdot \ln(1/T_o). \quad (1)$$

Then, the optical band gaps  $E_g$  were obtained via the following equation [15]:

$$(\alpha \cdot h\nu)^2 = A \cdot (h\nu - E_g), \quad (2)$$

where  $A$  is a constant and  $h\nu$  denotes the photon energy. The  $E_g$  value has been obtained graphically through an extrapolation of the linear portion of the  $(\alpha \cdot h\nu)^2$  dependence on  $h\nu$ .

The Urbach energy ( $E_0$ ), which originates from the optical transitions, assisted by sub-bandgap photons due to availability of a large number of point defects in the forbidden band was determined, in accordance with [16], by equation:

$$a = \alpha_0 \cdot \exp(h\nu / E_0), \quad (3)$$

where  $\alpha_0$  is a constant. According to [16], the structural disorder of the film was assessed from the  $E_0$  determined by fitting the linear portions of  $\ln(a)$  versus  $h\nu$ , namely, from the slope of the linear part of the dependence  $\ln(a)$  on  $h\nu$  near the band gap energy value.

To analyze phase compositions and structural parameters of ZnO layers, we recorded X-ray diffraction patterns by a DRON-4" diffractometer. Scanning was performed with Bragg-Brentano focusing ( $2\theta - 2\theta$ ). The resulting XRD patterns were processed and the profile parameters of the diffraction lines were calculated by New-Profile v.3.4 (486) and OriginPro v.7.5 software. The presence of crystalline phases was revealed by comparing the experimental diffraction patterns with the reference database JCPDS by using PCPDFWIN v.1.30 software. In accordance with [17], to evaluate crystallite size  $D$  and lattice microstrains induced mainly by point defects  $\varepsilon = \Delta d/d$  (where  $d$  is the crystal interplanar spacing according to JCPDS, and  $\Delta d$  is the difference between the corresponding experimental and reference interplanar spacings) we applied the X-ray line broadening method using the Scherrer's equation. Dislocation density was evaluated as  $1/D^2$  according to [18]. The crystal lattice constants,  $a$  and  $c$ , of the nanocrystalline ZnO grains were calculated using the least-squares method by UnitCell software on the basis of all recorded reflections in the X-ray diffraction patterns, as in [13]. Texture quality of ZnO layers was estimated by the Harris method [13]. Pole density  $P_i$ , which determines an axis of the crystal plane that is oriented normal to the surface, was calculated according to the equation [13]:

$$P_i = (I_i / I_{i0}) / \left[ 1 / N \sum_{i=1}^N (I_i / I_{i0}) \right], \quad (4)$$

where  $I_i$ ,  $I_{i0}$  are integral intensities of the  $i$ -th diffraction peak of the film and etalon, respectively;  $N$  is the number of lines presented in the diffraction. Texture axis has the index, which corresponds to the largest value of  $P_i$ . The orientation factor  $f$  for the relevant direction was calculated from the formula [19]:

$$f = \sqrt{1 / N \sum_{i=1}^N (P_i - 1)^2}. \quad (5)$$

### 3. RESULTS AND DISCUSSION

Fig. 1 demonstrates X-ray diffraction patterns of the 1D ZnO nanostructured arrays electrodeposited in the pulsed mode (a) and of the ZnO films obtained by SILAR technique (b) both before and after treatment in the glow-discharge hydrogen plasma. Analysis of XRD patterns has shown that regardless of the  $H_2^+$  plasma treatment all ZnO layers are single-phased, polycrystalline in nature and matching with hexagonal wurtzite structure ZnO (JCPDS 36-1451). As calculations of structural parameters have revealed (Table 1), ZnO layers are characterized by grain size in the range of 28-36 nm, revealing the nanocrystalline nature. Note that because of the small thickness of ZnO layers and due to their nanocrystalline structure, it was not possible to analyze ZnO substructural parameters in full. For this reason, Table 1 contains many dashes. However, according to the available data, the ZnO layers were grown along the axial texture [001] (the orientation factor in the (002) plane  $f$  near one a. u.) and have the dislocation densities from  $6.9 \cdot 10^{14}$  to  $1.5 \cdot 10^{15}$  lines/m<sup>2</sup>, the values similar to the obtained in [20] for nanocrystalline ZnO thin films were derived by advanced spray pyrolysis. We can see in Table 1 the increased microstrains  $\epsilon$  that are evidently related to the crystal lattice parameters,  $a$  and  $c$ , which are different from the reference data JCPDS 36-1451. In general, the XRD data (crystallite size, dislocation density, microstrains) show significant destructive effect of glow-discharge hydrogen plasma on structure of the electrodeposited 1D ZnO arrays. On the contrary, these indicators were even slightly improved after plasma treatment of zinc oxide films, which were produced by the SILAR method (Table 1). Paper [6] presents results of X-ray diffraction analysis, which show that structure of the hydrogen plasma treated aluminum doped ZnO (AZO) thin film with a thickness of 0.33  $\mu\text{m}$  deposited by radio frequency (RF) magnetron sputtering did not change, but its crystallinity deteriorated as compared to that of the as-deposited film due to hydrogen incorporation into AZO film. Thus, it can be assumed that the decrease in the grain size  $D$  with an increase in microstrains  $\epsilon$  and with growth of the dislocations in the electrodeposited 1D ZnO arrays after plasma treatment is a consequence of the hydrogen introduction into zinc oxide lattice, for example in the form of H-related defects. Similar effect of hydrogen plasma on crystal structure of magnetron sputtered nanostructured ZnO films is described in [7]. Formation of defects in zinc oxide due to the incorporation of hydrogen during hydrogen plasma processing was confirmed in a large number of works [1-6, 9, 21-23]. Besides, it should be noted that for the nanostructured zinc oxide surface in humid atmosphere and especially for ZnO layers obtained from aqueous solutions, it is characteristic a presence of Zn-O-H groups. As stated in [23], after hydrogen plasma treatment, these unstable Zn-O-H groups react with hydrogen ions, releasing  $H_2O$  and creating oxygen vacancies  $V_o$ . It is noted in [22] that  $V_o$  results in the occurrence of isolated energy levels, which significantly enhance the optical absorption, charge generation and separation. Moreover, the  $V_o$  in ZnO near the surface act as the active sites, which are

involved in the surface adsorption and reaction processes. For these reasons, there is a great interest in the development of controllable synthesis of ZnO nanomaterials with  $V_o$  and exploiting their unique properties and potential applications [22].

According to literary data [4], plasma treatment is one of the most effective methods for the surface modification of ZnO thin films and 1D nanostructures. It is noted in [21] that owing to RF glow-discharge hydrogen plasma treatment the magnetron sputtered AZO films are degraded by a simultaneous reduction of the oxide and vaporization of corresponding metal (Zn in the main) after the reduction. As it can be seen in the top view SEM images in Fig. 2a, b, there are significant changes in the surface morphology of ZnO/FTO sample with electrodeposited 1D ZnO array caused by glow-discharge hydrogen plasma processing. Probably, white dots in Fig. 2b are the areas where the zinc oxide was

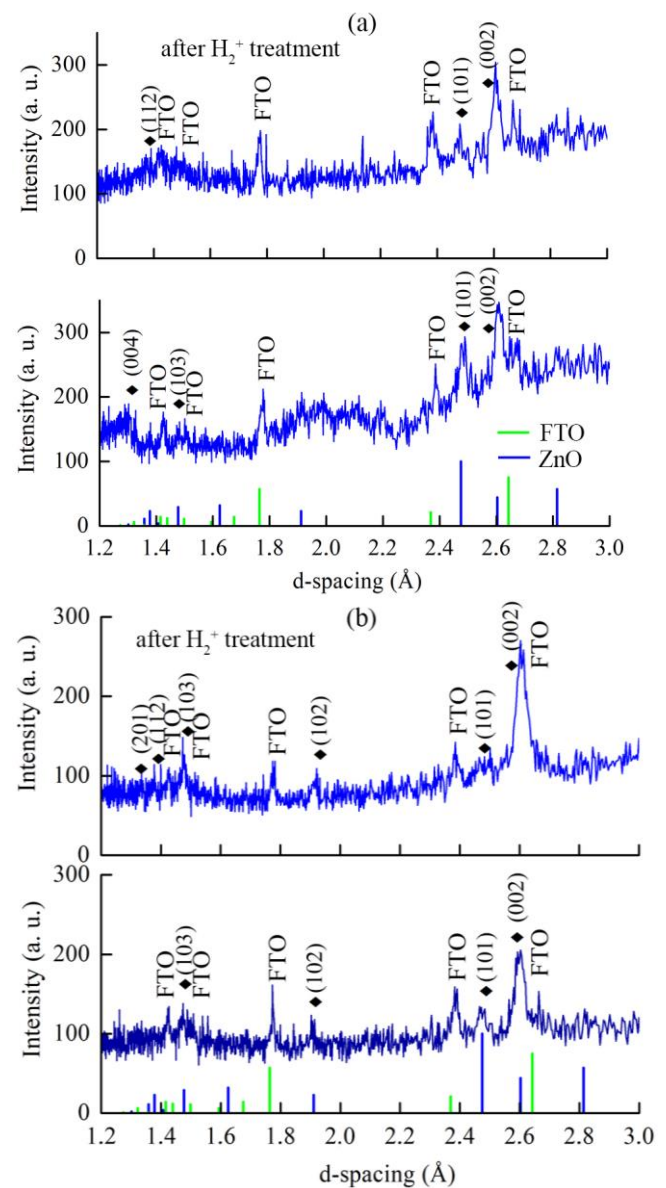
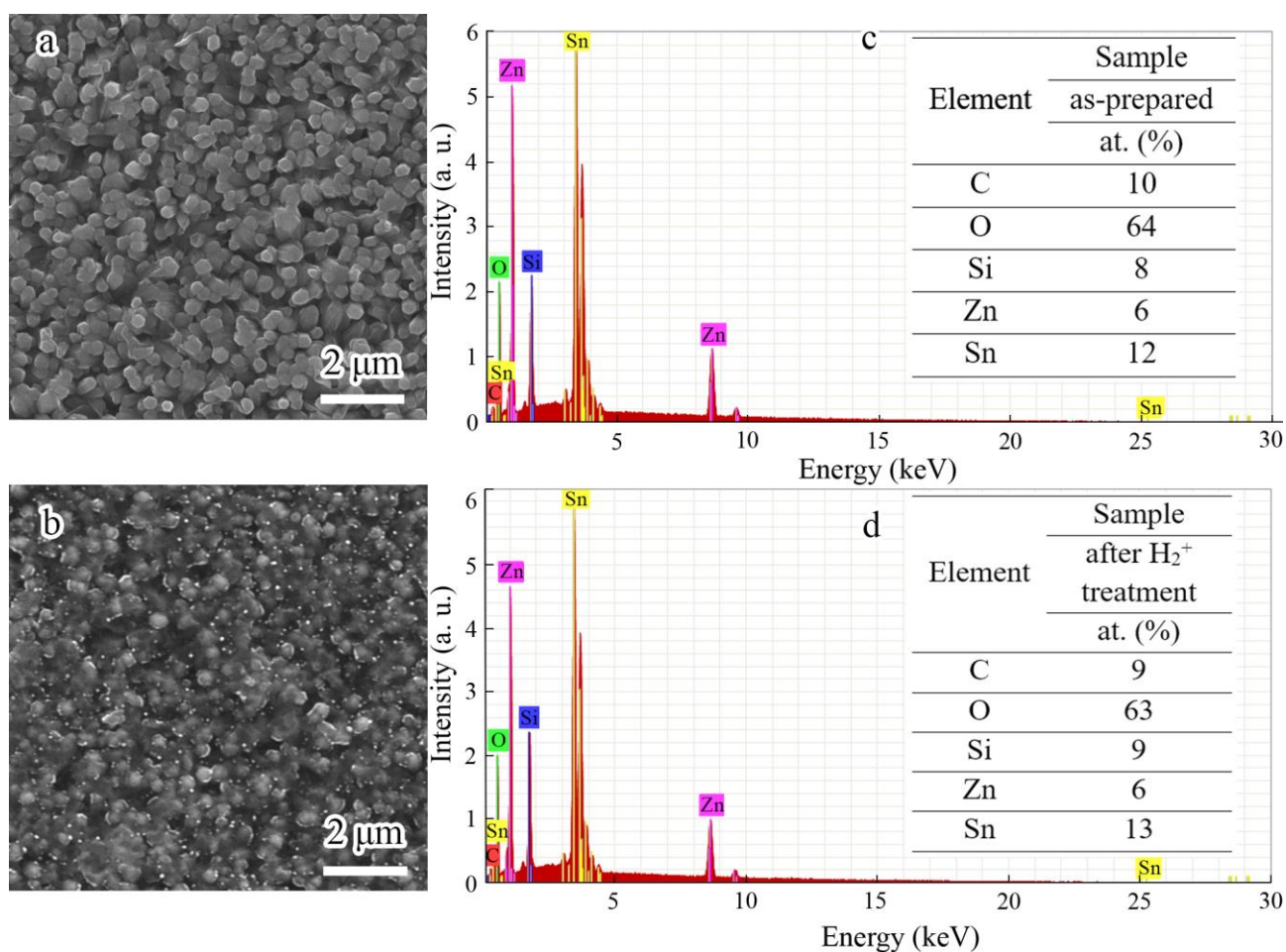


Fig. 1 – XRD patterns of the electrodeposited 1D ZnO arrays (a) and of the ZnO films obtained by SILAR technique (b) both before and after glow-discharge hydrogen plasma treatment

**Table 1** – Structural parameters of ZnO layers before and after treatment in the glow-discharge hydrogen plasma

Sample	Crystallite size $D$ , nm	Dislocation density, lines/m <sup>2</sup>	Microstrains $\varepsilon$ , 10 <sup>-3</sup> a. u.	Lattice parameters, Å		Texture		
				$a$	$c$	$hkl$	$P_{hkl}$	Orientation factor $f$
etalon ZnO (JCPDS 36-1451)	–	–	–	3.249	5.206	–	–	–
as-electrodeposited 1D ZnO array	38	6.9 · 10 <sup>14</sup>	3.4	–	–	(002)	3.3	1.3
electrodeposited 1D ZnO array after H <sub>2</sub> <sup>+</sup> treatment	26	1.5 · 10 <sup>15</sup>	5.0	–	–	–	–	–
ZnO film as-deposited by SILAR	26	1.5 · 10 <sup>15</sup>	5.0	–	–	–	–	–
ZnO film deposited by SILAR after H <sub>2</sub> <sup>+</sup> treatment	29	1.2 · 10 <sup>15</sup>	4.6	3.214	5.247	(002)	3.2	1.0

**Fig. 2** – Top view SEM images of the electrodeposited 1D ZnO arrays: as-prepared (a) and after the glow-discharge hydrogen plasma treatment (b). (c) X-ray fluorescence spectrum of as-electrodeposited 1D ZnO array; (d) X-ray fluorescence spectrum of the electrodeposited 1D ZnO array after H<sub>2</sub><sup>+</sup> treatment ( $t \approx 0.7 \mu\text{m}$ )

etched by the glow-discharge H<sub>2</sub><sup>+</sup> plasma from the electrodeposited 1D ZnO array surface. X-ray fluorescence spectra of the ZnO/FTO samples in Fig. 2c, d demonstrate a decrease of Zn content in the electrodeposited 1D ZnO array after glow-discharge H<sub>2</sub><sup>+</sup> plasma processing, as compared with Sn of FTO and with Si of glass. Probably, it is due to the reduction of zinc oxide

with evaporation of zinc from the 1D ZnO surface similar to that described in [21]. Apparently, this process is more significant for 1D ZnO arrays in hydrogen plasma treated ZnO/FTO samples than the occurrence of V<sub>o</sub> defects in accordance with [22, 23].

Comparison of top view SEM images of ZnO films produced by the SILAR method before and after glow-

discharge hydrogen plasma treatment in Fig. 3a and Fig. 3b, respectively, shows slight hydrogen plasma etching mainly along the edges of nanostructured ZnO films without their destruction. Chemical composition of ZnO/FTO samples with ZnO film deposited through SILAR method, which was determined by XRF microanalysis before and after glow-discharge  $H_2^+$  plasma processing, is shown in Fig. 3c and Fig. 3d, respectively. It is seen that ZnO film obtained by SILAR is thicker and denser than the electrodeposited 1D ZnO array, since the Zn content in its spectra is much higher than that of Sn from FTO and of Si from glass compared with 1D ZnO array both before and after plasma treatment. In addition, the relative content of Zn in the ZnO film deposited via SILAR increases after glow-discharge  $H_2^+$  plasma processing, probably because Zn-O-H groups in the ZnO film react with hydrogen ions, releasing  $H_2O$  and creating oxygen vacancies  $V_o$ . According to [22],  $c$ -axis expansion and  $a$ -axis compression of ZnO film deposited by SILAR after  $H_2^+$  treatment can be used as an indicator of the  $V_o$  concentration increase (Table 1). As stated in [22], these XRD data suggested that the unit cell of ZnO shrink perpendicular to the crystallographic  $c$ -axis with increasing formation of  $V_o$  due to hydrogen plasma processing and consequently the bond length between the  $Zn^{2+}$  ion and

the three non-axial oxygen atoms in the  $ZnO_4$  tetrahedra became shorter. Analysis of optical properties of the electrodeposited 1D ZnO array and of the obtained by the SILAR method ZnO film both before and after the glow-discharge hydrogen plasma treatment has revealed a decrease in transparency and reduction of diffuse reflectance in the visible spectrum for these films due to  $H_2^+$  plasma processing (Fig. 4). According to [22], it is due to the occurrence of  $V_o$  defects. If do not take into account the ring darkening in the photo in Fig. 4a, explained by the features of the equipment, which limits the  $H_2^+$  irradiated area of the 1D ZnO array surface, it appears that the central part of the inner spot darkened only slightly. This is confirmed by the optical transmission spectra in Fig. 4a. It can be assumed that the number of oxygen vacancies arising after hydrogen plasma treatment in the electrodeposited 1D ZnO array is less significant than 1D ZnO etching by  $H_2^+$  plasma. A more noticeable darkening due to plasma treatment is observed for ZnO films obtained by the SILAR method (photo in Fig. 4b). It corresponds to a much greater reduction in the optical transmittance of ZnO film after glow-discharge  $H_2^+$  plasma processing shown by  $T_o(\lambda)$  spectra in Fig. 4b.

According to [22], dark spot on the glow-discharge hydrogen plasma treated surface of the ZnO film made

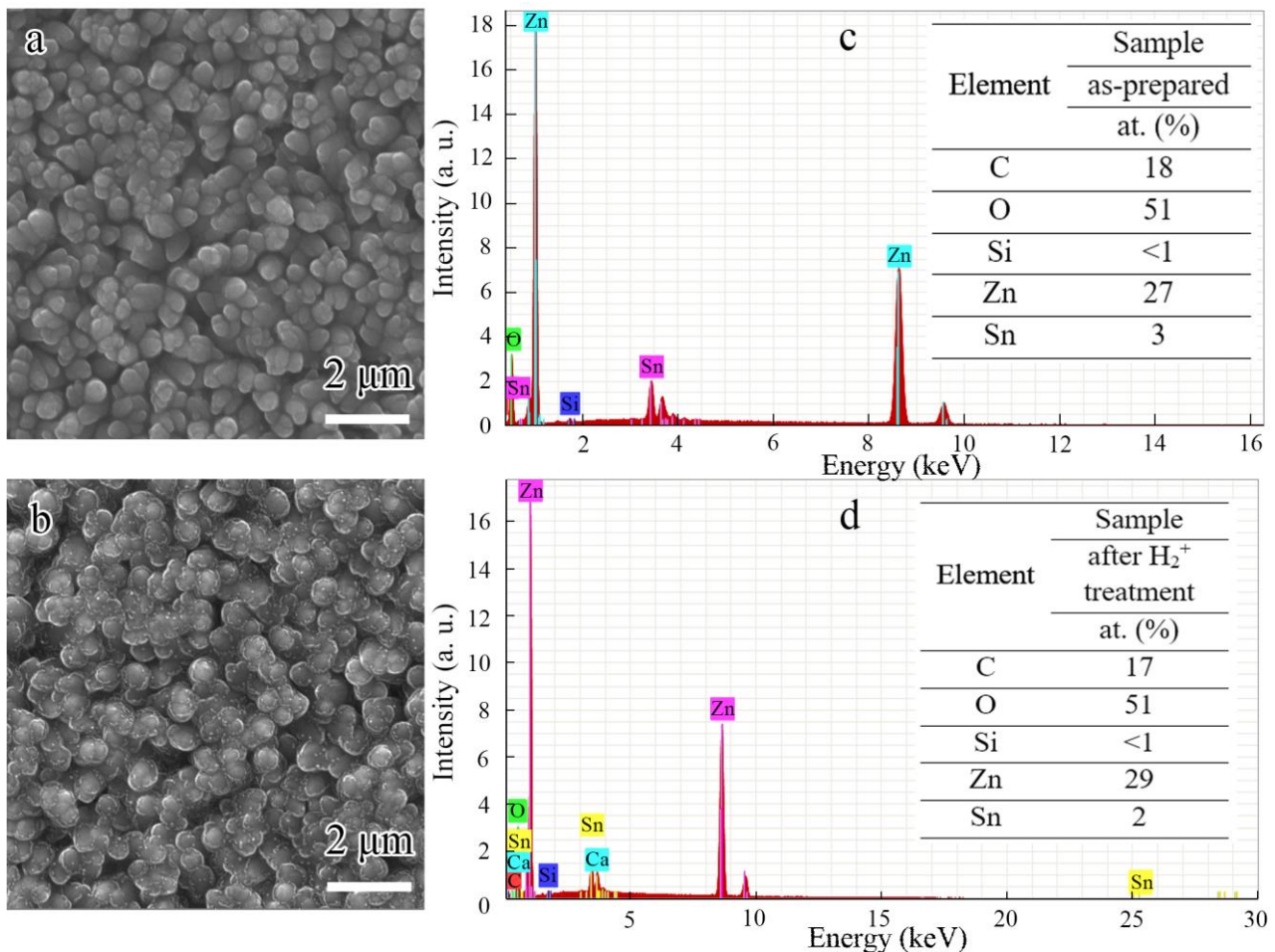


**Fig. 3** – Top view SEM images of the obtained by the SILAR method ZnO film: as-prepared (a) and after the glow-discharge hydrogen plasma treatment (b). (c) X-ray fluorescence spectrum of as-deposited via SILAR ZnO film; (d) X-ray fluorescence spectrum of the deposited via SILAR ZnO film after  $H_2^+$  treatment ( $t \approx 1 \mu m$ )

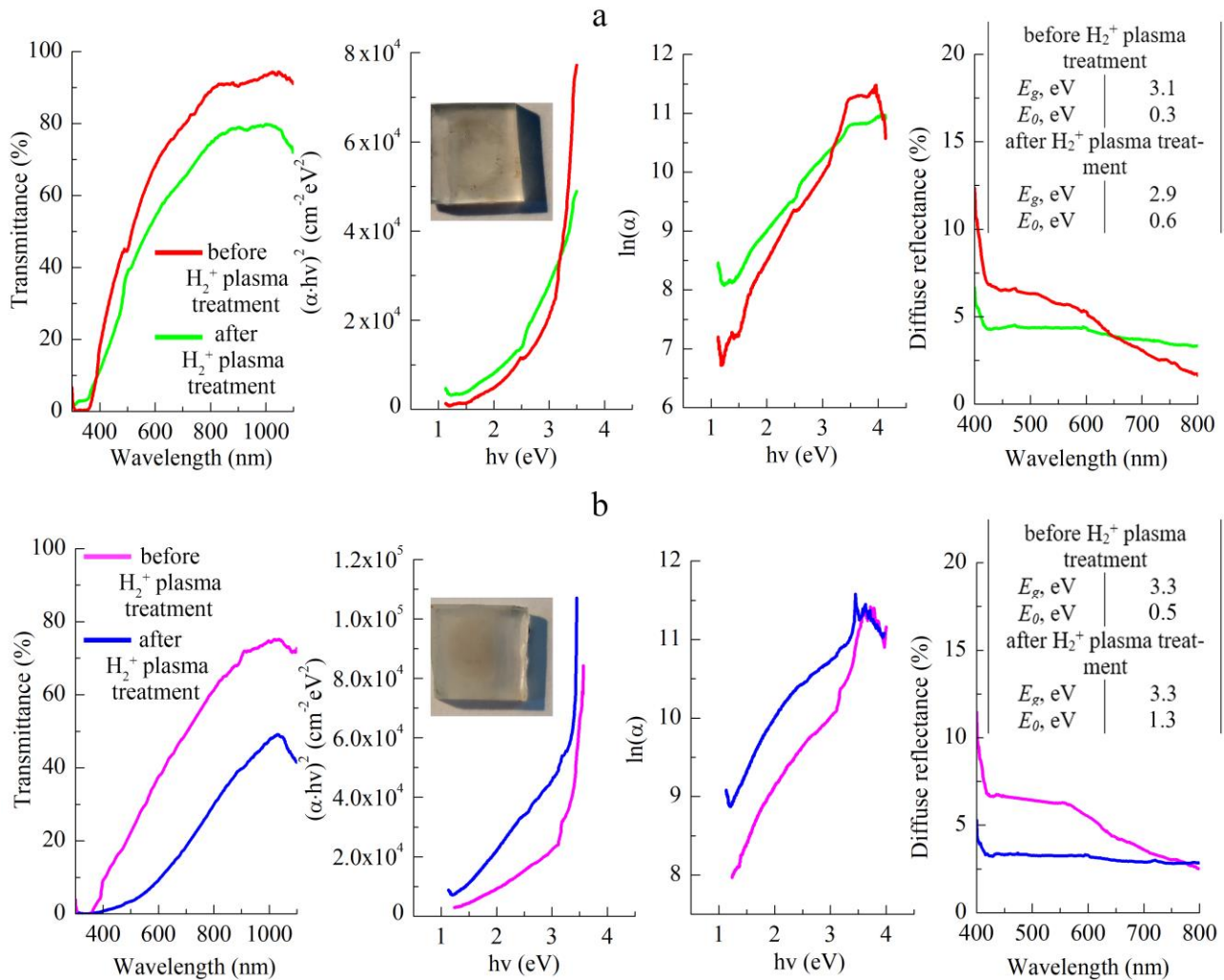


**Fig. 4** – (a) Optical properties of the electrodeposited 1D ZnO array as-prepared and after the glow-discharge hydrogen plasma treatment, and photo after  $H_2^+$  plasma treatment of a circular area in the middle of this ZnO/FTO sample surface. (b) Optical properties of the obtained by the SILAR method ZnO film as-prepared and after the glow-discharge hydrogen plasma treatment, and photo after  $H_2^+$  plasma treatment of a circular area in the middle of this ZnO/FTO sample surface

by the SILAR method (photo in Fig. 4b) is clear evidence of the appearance of a large number of  $V_o$  defects. As seen from  $(\alpha \cdot hv)^2$  dependences on  $h\nu$  for both 1D ZnO array and for the obtained by the SILAR method ZnO film, the hydrogen plasma processing leads to a decrease of optical band gaps. In addition to the  $E_g$  diminution, ZnO layers of both types exhibit after  $H_2^+$  plasma treatment a significant broadening of the Urbach tails. The analysis of the  $\ln(\alpha)$  versus  $h\nu$  dependences indicates an increase in the Urbach energy of both ZnO layers after exposure to glow-discharge hydrogen plasma. All three observations listed above are, according to [22], evidence of the appearance of oxygen vacancies in the ZnO layers.

#### 4. CONCLUSIONS

Studies have shown that regardless of the  $H_2^+$  plasma treatment, all ZnO layers prepared through pulsed electrochemical deposition and via SILAR method are single-phased, polycrystalline in nature and matching with hexagonal wurtzite structure ZnO. A common feature for the zinc oxide layers of both types is the appear-

ance of oxygen vacancies  $V_o$  under the influence of hydrogen plasma. In addition to structural characteristics (an increase in the Urbach energy,  $c$ -axis expansion,  $a$ -axis compression), the creation of  $V_o$  is manifested in the decrease in transparency and diffuse reflectance, as well as in the narrowing optical band gap of ZnO. Besides, we recorded in the electrodeposited 1D ZnO arrays after glow-discharge hydrogen plasma treatment the decrease in the grain size with an increase in microstrains and with growth of the dislocations. The probable cause is the hydrogen introduction into ZnO, for example in the form of H-related defects. Additionally, zinc oxide was etched by the glow-discharge  $H_2^+$  plasma through its reduction and evaporation of Zn from the surface, especially from the electrodeposited 1D ZnO array surface.

On the whole, investigations of effect of glow-discharge hydrogen plasma treatment on zinc oxide layers prepared through pulsed electrochemical deposition and via SILAR method show their quite good stability to the plasma-induced radiation and chemical impacts under high total  $H_2^+$  fluence received by every ZnO/FTO sample  $\sim 8 \cdot 10^{18} \text{ cm}^{-2}$ .

## REFERENCES

- J.J. Dong, X.W. Zhang, J.B. You, P.F. Cai, Z.G. Yin, Q. An, X.B. Ma, P. Jin, Z.G. Wang, P.K. Chu, *ACS Appl. Mater. Interfaces* **2**, 1780 (2010).
- J.B. You, X.W. Zhang, P.F. Cai, J.J. Dong, Y. Gao, Z.G. Yin, N.F. Chen, R.Z. Wang, H. Yan, *Appl. Phys. Lett.* **94**, 262105 (2009).
- P.F. Cai, J.B. You, X.W. Zhang, J.J. Dong, X.L. Yang, Z.G. Yin, N.F. Chen, *J. Appl. Phys.* **105**, 083713 (2009).
- W.-K. Hong, J. Yoon, T. Lee, *Nanotechnology* **26**, 125202 (2015).
- V. Papamakarios, E. Polydorou, A. Soultati, N. Droseros, D. Tsikritzis, A.M. Douvas, L. Palilis, M.Fakis, S. Kennou, P. Argitis, M. Vasilopoulou, *ACS Appl. Mater. Interfaces* **8**, 1194 (2016).
- F.-H. Wang, H.-P. Chang, C.-C. Tseng, C.-C. Huang, H.-W. Liu, *Current Appl. Phys.* **11**, S12 (2011).
- P.-W. Chi, C.-W. Su, D.-H. Wei, *Sci. Reports* **7**, 43281 (2017).
- Y.-Y. Chang, J. Stuchlík, N. Neykova, J. Souček, Z. Remeš, *J. Electrical Eng.* **68**, 70 (2017).
- C.-C. Lin, H.-P. Chen, H.-C. Liao, S.-Y. Chen, *Appl. Phys. Lett.* **86**, 183103 (2005).
- M. Gruntman, *J. Geophys. Res.: Space Phys.* **101**, 15555 (1996).
- A. Bogaerts, *J. Anal. At. Spectrom.* **14**, 1375 (1999).
- S. Bose, A.K. Barua, *J. Phys. D: Appl. Phys.* **32**, 213 (1999).
- V.R. Kopach, K.S. Klepikova, N.P. Klochko, I.I. Tyukhov, G.S. Khrypunov, V.E. Korsun, V.M. Lyubov, A.V. Kopach, R.V. Zaitsev, M.V. Kirichenko, *Sol. Energy* **136**, 23 (2016).
- M.A. Desai, A.N. Vyas, G.D. Saratale, S.D. Sartale, *Int. J. Hydrogen Energy* **44**, 2091 (2019).
- S.Y. Park, K. Kim, K.-H. Lim, B.J. Kim, E. Lee, J.H. Cho, Y.S. Kim, *J. Mater. Chem. C* **1**, 1383 (2013).
- M. Chávez, H. Juárez, M. Pacio, X. Mathew, R.G.L. Chaltel, M. Zamora, O. Portillo, *Revista Mexicana de Física* **62**, 124 (2016).
- A.K. Zak, W.H.A. Majid, M.E. Abrishami, R. Yousefi, *Solid State Sci.* **13**, 251 (2011).
- M. Dongol, A. El-Denglawey, M.S. Abd El Sadek, I.S. Yahia, *Optik* **126**, 1352 (2015).
- N.P. Klochko, V.R. Kopach, I.I. Tyukhov, D.O. Zhadan, K.S. Klepikova, G.S. Khrypunov, S.I. Petrushenko, V.M. Lyubov, M.V. Kirichenko, S.V. Dukarov, A.L. Khrypunova, *Solar Energy* **164**, 149 (2018).
- P.S. Shewale, G.L. Agawane, S.W. Shin, A.V. Moholkar, J.Y. Lee, J.H. Kim, M.D. Uplane, *Sens. Actuat. B* **177**, 695 (2013).
- T. Minami, H. Sato, H. Nanto, S. Takata, *Thin Solid Films* **176**, 277 (1989).
- J. Wang, R. Chen, L. Xiang, S. Komarneni, *Ceramics Int.* **44**, 7357 (2018).
- Y. Jeong, C. Pearson, Y.U. Lee, K. Ahn, C.-R. Cho, J. Hwang, H. Kim, L.-M. Do, M.C. Petty, *J. Appl. Phys.* **116**, 074509 (2014).

### Вплив обробки у водневій плазмі тліючого розряду на шари оксиду цинку, виготовлені імпульсним електрохімічним осадженням і методом SILAR

Н.П. Ключко<sup>1</sup>, К.С. Клепікова<sup>1</sup>, С.І. Петрушенко<sup>2</sup>, А.В. Нікітін<sup>3</sup>, В.Р. Копач<sup>1</sup>, І.В. Хрипунова<sup>1</sup>, Д.О. Жадан<sup>1</sup>, С.В. Дукаров<sup>2</sup>, В.М. Любов<sup>1</sup>, А.Л. Хрипунова<sup>1</sup>

<sup>1</sup> Національний технічний університет «Харківський політехнічний інститут», вул. Кирпичова, 2, 61002 Харків, Україна

<sup>2</sup> Харківський національний університет імені В.Н. Каразіна, пл. Свободи, 4, 61022 Харків, Україна

<sup>3</sup> Національний науковий центр «Харківський фізико-технічний інститут», вул. Академічна, 1, 61108 Харків, Україна

У роботі ми досліджували вплив обробки в плазмі тліючого розряду  $H_2^+$  на шари  $ZnO$ , які були нанесені на покриті плівками легованого фтором оксиду олова (FTO) скляні підкладки шляхом низькотемпературного осадження з водних розчинів, а саме, методом імпульсного електрохімічного осадження і методом послідовної адсорбції і реакції іонних шарів (SILAR). Показано, що кристалічна структура, морфологія поверхні, хімічний склад і оптичні властивості після плазмової обробки зазнають деяких деструктивних змін через утворення кисневих вакансій  $V_o$  і пов'язаних з воднем дефектів, а також внаслідок того, що  $H_2^+$ -плазма тліючого розряду здатна травити  $ZnO$  шляхом відновлення оксиду цинку і випаровування з поверхні  $Zn$ . Проте в цілому, наші дослідження продемонстрували досить добру стійкість шарів  $ZnO$  до радіаційного та хімічного впливів плазми при одержаній кожним зразком  $ZnO/FTO$  високій сумарній густині потоку  $H_2^+$  приблизно  $8 \cdot 10^{18} \text{ см}^{-2}$ .

**Ключові слова:** Тліючий розряд, Оксид цинку, Імпульсне електроосадження, SILAR, Воднева плазма обробка.